

Expression of the NMDA receptor subunit GluN3A (NR3A) in the olfactory system and its regulatory role on olfaction in the adult mouse

Jin Hwan Lee^{1,3} · Ling Wei^{1,2} · Todd C. Deveau¹ · Xiaohuan Gu^{1,3} · Shan Ping Yu^{1,3}

Received: 5 March 2015 / Accepted: 25 August 2015 / Published online: 3 September 2015
© Springer-Verlag Berlin Heidelberg 2015

Abstract Glutamate is an excitatory neurotransmitter in the olfactory system and its *N*-methyl-D-aspartate-(NMDA) receptor subunits [GluN1 (NR1), GluN2A (NR2A), and GluN2B (NR2B)] are expressed at synapses in the olfactory bulb and olfactory epithelium. Thus, glutamatergic neurons and NMDA receptors play key roles in olfaction. GluN3A (NR3A) is a unique inhibitory subunit in the NMDA receptor complex; however, the expression and functional role of GluN3A in the olfactory bulb and epithelium remain unclear. The present study examined the expression patterns of GluN3A in the olfactory bulb and epithelium and explored its functional role in the olfactory system. Immunohistochemical and Western blot analyses revealed that GluN3A is abundantly expressed in different cellular layers of the olfactory bulb and epithelium of the adult wild type (WT) mice. In littermate GluN3A knockout (GluN3A^{-/-}; KO) mice, the expression of olfactory marker protein normally found in mature olfactory sensory neurons was significantly reduced in the olfactory bulb and epithelium. A butyl alcohol stimulus increased immediate-early gene *c-Fos* expression in the olfactory system of WT mice, while this response was absent in GluN3A KO mice. The level of phosphorylated Ca²⁺/calmodulin-dependent kinase II was significantly lower in GluN3A KO mice compared to WT mice. In buried food

finding test, GluN3A mice took significantly longer time to find food compared to WT mice. Consistently, impaired odor distinguishing ability was seen in GluN3A KO mice. These findings suggest that GluN3A, expressed in the adult olfactory system, plays a significant regulatory role in olfactory development and functional activity.

Keywords NMDA · GluN3A (NR3A) · Olfaction · Olfactory bulb · Olfactory epithelium

Abbreviations

NMDA	<i>N</i> -methyl-D-aspartate
NMDAR	NMDA receptor
WT	Wild-type
KO	Knockout
GluN1	Glutamate NMDA receptor 1 (NR1)
GluN2	Glutamate NMDA receptor 2A (NR2A)
GluN2B	Glutamate NMDA receptor 2B (NR2B)
GluN3A	Glutamate NMDA receptor 3A (NR3A)
GluN3B	Glutamate NMDA receptor 3B (NR3B)
OMP	Olfactory marker protein
ONL	Olfactory nerve layer
GCL	Granular cell layer
MCL	Mitral cell layer
EPL	External plexiform layer
GL	Glomerular layer
CaMKII	Ca ²⁺ /calmodulin-dependent kinase II
CREB	CAMP response element-binding protein

✉ Shan Ping Yu
spyu@emory.edu

¹ Department of Anesthesiology, Emory University School of Medicine, 101 Woodruff Circle, WMB suite 620, Atlanta, GA 30322, USA

² Department of Neurology, Emory University School of Medicine, Atlanta, GA 30322, USA

³ Center for Visual and Neurocognitive Rehabilitation, VA Medical Center, Decatur, GA 30033, USA

Introduction

Glutamate mediates the majority of excitatory synaptic transmission in the central nervous system (CNS) (Mel-drum 2000). Glutamate acts on ionotropic and

metabotropic receptors that are widely expressed throughout the brain. The ionotropic glutamate receptors can be divided into three receptor groups: kainic acid receptors (or kainate receptors), α -amino-3-hydroxy-5-methyl-4-isoxazolepropionic acid (AMPA) receptors (AMPA receptors), and *N*-methyl-D-aspartate (NMDA) receptors (NMDARs) (Hollmann and Heinemann 1994). Among these receptors, NMDARs have received considerable attention because of their widespread distribution and broad functional role including brain development, neural plasticity, cognitive functions, excitotoxicity, and it also plays a role in many neurodegenerative diseases (Dingledine et al. 1999; Cull-Candy et al. 2001; Choi 1992).

NMDARs are composed of hetero-tetramers of subunits GluN1, GluN2, and may also include GluN3. While exact stoichiometry of hetero-multimers is still being elucidated, several facets suggest the possibility of NMDARs with a tetrameric composition. Additionally, tri-heteromeric GluN3-containing NMDARs could contain as few as 1 GluN2 subunit, and some evidence exists for GluN2-lacking, GluN1/GluN3 di-heteromeric receptors (Dingledine et al. 1999; McBain and Mayer 1994; Pabba et al. 2012). GluN1 is widely expressed in the CNS and is required for the fundamental formation of functional NMDARs (Dingledine et al. 1999; Laurie and Seeburg 1994). The GluN2 subunit is a key player in different functional properties of NMDAR complexes (Monyer et al. 1992). For example, the GluN2B subunit plays important roles in learning and memory via regulation of long-term potentiation (LTP) and long-term depression (LTD) (Bliss and Collingridge 1993).

The GluN3A subunit is an inhibitory NMDAR subunit which, when assembled with GluN1 and GluN2, reduces the Ca^{2+} permeability as well as the overall current generated by GluN1/GluN2 formed receptors (Perez-Otano et al. 2001). GluN3A expression is widely observed in brain regions such as the cerebral cortex, hippocampus, and thalamus (Ciabarra et al. 1995; Sucher et al. 1995). It was noted that GluN3 is only abundantly expressed during the neonatal stage, reaching a peak level in the rodent brain around postnatal days 7 through 10 and the expression declines to a much low level during adulthood (Ciabarra et al. 1995; Al-Hallaq et al. 2002). Based on this observation, research on GluN3A has been almost exclusively focused on the developing brain of neonates. It was shown that dendritic spine densities increased in the brains of young GluN3A KO mice, suggesting a role in synaptic development and neural plasticity (Das et al. 1998). On the other hand, we recently demonstrated that even though the GluN3A expression level is down regulated from the neonatal period, significant protein levels of GluN3A are still detectable in the adult brain. The presence of GluN3A

in the adult brain has some profound impacts on locomotor activity, pain sensation, and cognitive functions (Mohamad et al. 2013). Moreover, previous reports showed relatively high mRNA levels of GluN3 (NMDAR-L) in the olfactory system compared to other parts of the adult brain (Sucher et al. 1995). We propose in the present investigation that the expression of GluN3A in the adult brain, particularly in the olfactory system, should not be overlooked and a better understanding of its physiological and pathological roles is fundamentally important and necessary.

Olfactory function requires sequential and hierarchical stages of neuronal organization through which chemical sensory input is processed (Shepherd 2004). When odors are inhaled through the nasal passages, they bind to the class A rhodopsin-like G protein-coupled receptors (GPCRs) of olfactory sensory neurons (Firestein 2001). The odor signal is then transferred into the piriform cortex and other central regions (e.g. frontal cortex, hippocampus, and amygdala, etc.) via the olfactory bulb (Margot 2009). This process transforms the olfactory signal from a molecular signal into complex neuronal activity. Previous investigations have shown that NMDA receptors such as GluN1, GluN2A, and GluN2B are expressed in the granular cell layer, mitral cell layer, and tufted cell layer of the olfactory bulb. Glutamate released from mitral cells initiates a prolonged excitation and inhibitory GABA_A receptor currents in the same mitral cell (Isaacson and Strowbridge 1998; Schoppa et al. 1998), which are the events coupling Ca^{2+} influx through the NMDA receptor to GABA release at the reciprocal dendro-dendritic synapse (Halabisky et al. 2000; Isaacson 2001; Chen et al. 2000). These results suggested that NMDAR activity plays an important role in olfaction.

Although a few earlier studies on the distribution of GluN3A in the neonatal brain mentioned GluN3A expression in the olfactory bulb (Sucher et al. 1995; Wong et al. 2002), little is known to date about the specific cellular distribution and putative functional roles of GluN3A in the adult olfactory system, including the olfactory bulb and olfactory epithelium. Based on our previous investigations showing functional roles of GluN3A in synaptic plasticity associated with sensorimotor activities and cognitive functions of the adult brain (Mohamad et al. 2013), the present investigation tested the hypothesis that GluN3A is an imperative regulatory player in olfactory function of the adult brain. To study this hypothesis, morphological and functional evidence were compared between wild type (WT) and GluN3A knockout (KO) mice. Our data support the idea that GluN3A is a significant NMDAR subunit that exhibits important functional roles not only in neonates but also in adult animals.

Materials and methods

WT and GluN3A KO mice

All animal experiments and experimental protocols were approved by the Emory University Institutional Animal Care and Use Committee (IACUC) and were in compliance with National Institutes of Health (NIH) guidelines. GluN3A KO (GluN3A^{-/-}) mice and WT counterparts were originally provided by Nobuki Nakanishi and Stuart A. Lipton at Sanford-Burnham Medical Research Institute (La Jolla, California, USA); detailed information of the background of these mice was described previously (Das et al. 1998). Briefly, embryonic stem cells derived from 129/SvJ were electroporated with DNA carrying disrupted GluN3A gene and then injected into blastocysts from C57BL/6 mice. The resulting chimeric males were crossed with BlackSwiss or 129SvEv females to produce F1 heterozygotes. GluN3A KO homozygote mice were then produced by cross-breeding F1 mice. In our lab, homozygote colonies of either WT or GluN3A KO mice were maintained under the same conditions with identical animal care environment. All animals were kept in air-conditioned rooms of 12-h light/dark cycle at temperature of 22 °C, with free access to same food and water supply except when food was restricted the day before olfaction testing. Littermate WT and KO animals were tested in the experiments.

Genotyping of animals

The Genotyping of WT and KO animals was performed as described previously (Mohamad et al. 2013). DNA for genotyping was extracted from tail snips (approximately 2–4 mm). Two separate sets of primers were used for the GluN3A KO and WT mice, respectively. For the WT reaction, the forward primer was: 5'-CCACGGTGAGCTTGGGGAAG-3' and the reverse primer was: 5'-TTGGGGA GCGCCCTGCATGG-3'. For the KO reaction, the forward primer was: 5'-CCACGGTGAGCTTGGGGAAG-3' and the reverse primer was: 5'-GCCTGAAGAACGAGATCA GG-3'. DNA (2 µl) was amplified on a thermocycler (MJ mini, Personal Thermal Cycler, Bio-Rad, CA, USA) for 40 cycles (95 °C for 60 s, 58 °C for 30 s, 72 °C for 60 s). After additional incubation at 72 °C for 10 min and transferred to 4 °C, PCR products were subjected to electrophoresis in 1.5 % agarose gel with ethidium bromide. Relative intensity of PCR bands was analyzed using the InGenius3 manual gel system (Syngene, Frederick, MD, USA).

Western blot analysis

Brain tissues were lysed in a lysis buffer containing 0.02 M Na₄P₂O₇, 10 mM Tris-HCL (pH 7.4), 100 mM NaCl,

1 mM EDTA (pH 8.0), 1 % Triton, 1 mM EGTA, 2 mM Na₃VO₄, and protease inhibitor cocktail (Sigma-Aldrich, St. Louis, MO, USA). The supernatant was collected after centrifugation at 15,000×g for 10 min at 4 °C. Protein concentration was determined with a standard bicinchoninic acid (Pierce Biotechnology, Rockford, IL, USA) assay. Protein was normalized and equivalent amounts of total protein were separated by molecular weight on SDS-polyacrylamide gradient gel, and then transferred to PVDF membranes. The blot was incubated in 5 % bovine serum albumin (Sigma-Aldrich) for 1 h and then reacted with primary antibodies at 4 °C for overnight.

The primary antibodies used in this investigation included: rabbit anti-GluN1 antibody (1:2000; Cell Signaling, Danvers, MA, USA), rabbit anti-GluN2B antibody (1:2000; Cell Signaling), rabbit anti-GluN3A antibody (1:500; Abcam, Cambridge, MA, USA), rabbit anti-GluN3B antibody (1:2500; Millipore, Billerica, MA, USA), rabbit anti-c-Fos antibody (1:2000; Millipore), rabbit anti-CREB antibody (1:2000; Cell Signaling), rabbit anti-phosphorylated CREB antibody (1:2000; Cell Signaling), rabbit anti-CaMKII antibody (1:2000; Cell Signaling), rabbit anti-phosphorylated CaMKII antibody (1:2000; Cell Signaling), and mouse anti-actin (Sigma-Aldrich). After washing with TBST, membranes were incubated with AP-conjugated or HRP-conjugated secondary antibodies (GE Healthcare, Piscataway, NJ, USA) for 2 h at room temperature. After final washing with TBST, the signals were detected with bromochloroindolylphosphate/nitroblue tetrazolium (BCIP/NBP) solution (Sigma-Aldrich) or film. Signal intensity was measured by ImageJ (NIH, Bethesda, MD, USA) and normalized to the actin signal intensity.

Immunohistochemical staining of the olfactory system

Frozen brain tissues were sliced into 10 µm-thick coronal sections using a cryostat (Leica CM 1950; Leica Microsystems, Buffalo Grove, IL, USA). Sections were dried on the slide warmer for 30 min, fixed with 10 % formalin buffer, washed with -20 °C pre-cooled ethanol: acetic acid (2:1) solution for 10 min, and finally permeabilized with 0.2 % Triton-X 100 solution for 5 min. All slides were washed 3 times with PBS (5 min each) after each step. Then, tissue sections were blocked with 1 % fish gelatin (Sigma-Aldrich) in PBS for 1 h at room temperature, and subsequently incubated with the primary antibodies GluN3A (1:200; Abcam), OMP (1:400; Wako Chemicals, Richmond, VA, USA), c-Fos (1:500; Millipore), and NeuN (1:300; Millipore) overnight at 4 °C. Next day, slides were washed 3 times with PBS for 5 min, then reacted with the secondary antibodies Alexa Fluor[®]488 goat anti-mouse (1:300; Life Technologies, Grand Island,

NY, USA) and Cy3-conjugated donkey anti-rabbit (1:300; Jackson ImmunoResearch Laboratories, West Grove, PA, USA) or Cy5-conjugated donkey anti-mouse or rabbit (1:400; Jackson ImmunoResearch Laboratories) for 80 min at room temperature. For c-Fos detection in olfactory epithelium, DAB staining was also used. After 3 washes with PBS, nuclei were stained with Hoechst 33342 (1:20,000; Molecular Probes) for 5 min as a counterstain, then mounted with Vectashield mounting medium (Vector Laboratory, Burlingame, CA, USA), and coverslipped for microscopy and image analysis.

Glomeruli diameter measurement

To study glomeruli diameter, glomeruli labeled by OMP were randomly selected per brain section. Six sections were randomly selected for each animal and 6 glomeruli per section were analyzed in the glomerular layer of olfactory bulb. Glomeruli diameter was estimated by measuring the diameter perpendicular to the center of the maximum diameter of the glomeruli.

Cell counting

Cell counting was performed following the principles of design based stereology. Systematic random sampling was employed to ensure accurate and non-redundant cell counting. Every section under analysis was at least 90 μm away from the next. Three 10 μm thick sections, frozen, spanning the entire region of interest were selected for cell counting. Counting was performed on 6 non-overlapping randomly selected 20 \times or 40 \times fields per section.

Butyl alcohol exposure

Each WT and GluN3A KO mouse was transferred into a clean cage prior to exposure. After habituation for 30 min, the mouse was exposed to 10 % butyl alcohol (Sigma-Aldrich) for 15 min. Immediately after exposure, the mouse was killed to measure c-Fos expression in the brain.

Buried and visible food finding tests

A buried food-finding test was performed to assess the ability of animals to smell volatile odors (Yang and Crawley 2009; Jamain et al. 2008). Briefly, mice were fasted 24 h before testing and then individually placed into a fresh cage (37.5 \times 17 \times 18 cm) with standard bedding for 20 min. Chocolate chips were hidden 1 cm below and surface of bedding in a corner of the test cage. The tested mouse was positioned in the opposite corner, and the latency to find the food was recorded using a timer. Animals were subjected to this test without prior similar tests,

in order to prevent the confounding factor of spatial memory. The test was performed during a 5 min period. Mice were removed from the cage immediately when food was uncovered. The visible food-finding test was performed as a control to assess how significant the locomotor ability could influence the speed for animals to detect and reach to food. It was done 1 h after buried food finding test in the same day. The pellet was randomly placed on the top of the bedding. Animal activities were monitored during the tests using a top scan system (Clever Sys Inc., Reston, VA, USA). After finishing the 5-min recording, the videos were off-line analyzed by the TopScan Realtime Option Version 3.0 software (Clever Sys Inc.).

Olfactory habituation/dishabituation test

The olfactory habituation/dishabituation test was performed to test whether the animal could detect and differentiate different odors, including both non-social odors and social odors (Yang and Crawley 2009). The animals were initially presented with water for 2 min. After a 2 min interval, this was repeated until water was presented 3 times. After another 2 min interval a novel chocolate was presented for 2 min. This was repeated until chocolate was 3 times. Lastly, after another 2 min interval a novel almond was presented for 2 min. Almond was then presented for the total of 3 times. During all odorant presentations, a blind observer recorded the animals' interest for the odorant. Interest was defined as the bouts of sniffing to investigate the object with its snout within 2–3 cm from the object. In this test, we placed the odor soaked papers beyond animals' grasp to minimize the contamination. An animal with an olfactory impairment is predicted to show smaller or no differences in its interests between odors.

Home cage behavioral tests

Behavioral changes of experimental mice were monitored and analyzed using the home cage system (Clever Sys Inc.). Four cameras of the system can spontaneously monitor 4 cages, and each cage (191 mm \times 292 mm \times 127 mm) contained one mouse. The behavioral patterns were continuously recorded for 24 h. After finishing the recording, the videos were analyzed by the Home Cage Software 3.0 (Clever Sys Inc.).

Statistical analysis

GraphPad Prism 6 (GraphPad Software, San Diego, CA, USA) was used for statistical analysis. Student's two-tailed *t* test was used for the comparison of 2 groups, and One-way ANOVA followed by Bonferroni correction was used for multiple-group comparisons. Two-way ANOVA

followed by Bonferroni correction was used for repeated measurements. Significant differences between groups were identified by a P value of <0.05 . All data are presented as mean \pm SEM.

Results

GluN3A expression patterns in the olfactory bulb of adult mice

Immunohistochemical staining was applied to examine the distribution of GluN3A expression in the olfactory system of the adult mouse brain. GluN3A expression in WT mice showed distinct laminar and cellular specific features in the olfactory bulb (Fig. 1a). High levels of GluN3A immunoreactivity were observed in the granular cell layer (GCL), mitral cell layer (MCL), and glomerular layer (GL) of the olfactory bulb. At the cellular level, GluN3A mainly expressed in the cell body of the larger neurons in the mitral cell layer, which are the major projection neurons of the olfactory bulb (Fig. 1a). Lower levels of GluN3A immunoreactivity were detected in olfactory nerve layer (ONL) and external plexiform layer (EPL) (Fig. 1a). These results showed that GluN3A had a distinct expression pattern in the olfactory bulb and raised the possibility that GluN3A could be involved in odor signal transduction. We also observed co-labeling of NeuN and GluN3A in the GCL and MCL, suggesting GluN3A is expressed in neurons (Fig. 1b). GluN3A immunoreactivity in the olfactory bulb was not detected in GluN3A KO mice (Fig. 1c).

In Western blot analysis, we confirmed that the GluN1 and GluN2B subunits in the olfactory bulb were not significantly different between WT and GluN3A KO mice (Fig. 1d, f, g). As expected, the expression of GluN3A was largely eliminated in the brain of KO mice (Fig. 1e, h). Unlike GluN3A, there were similar levels of GluN3B between WT and GluN3A KO mice (Fig. 1d, i).

Expression of the olfactory marker protein (OMP) in the olfactory system of WT and GluN3A KO mice

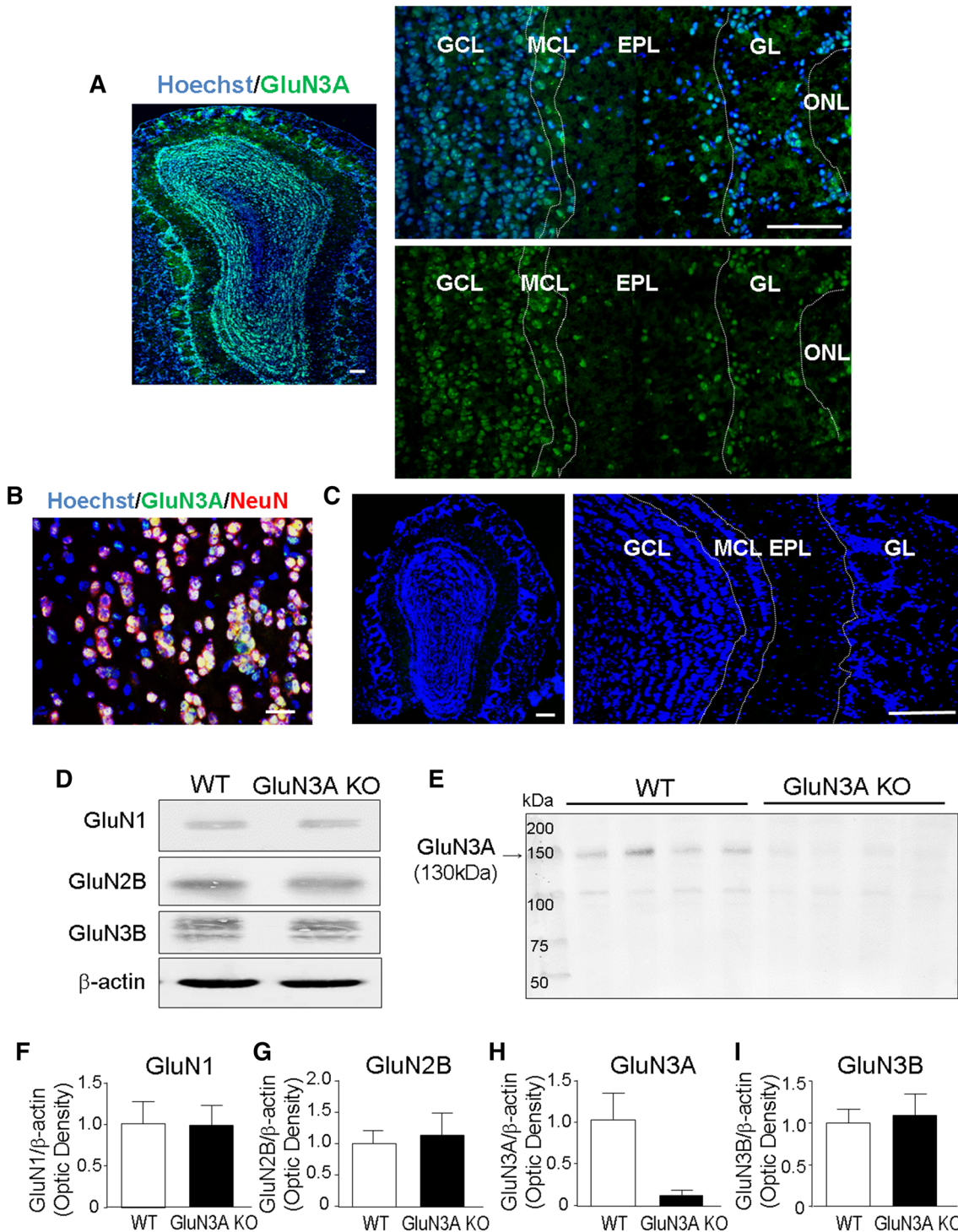
To understand whether GluN3A expression may affect olfactory development and functionality, we examined the expression of olfactory marker protein (OMP), a cytoplasmic protein in mature OSNs critical for the olfactory signal transduction cascade (Baldisseri et al. 2002; Margot 2009; Smith et al. 2002). In the sections containing the olfactory bulb, immunostaining in WT animals revealed abundant OMP expression in the ONL layer and GL layer of the olfactory bulb (Fig. 2a). Higher magnification of individual glomeruli verified co-expression of GluN3A

with OMP in OSNs (Fig. 2a). On the other hand, the brain sections from GluN3A KO mice displayed lower expression of OMP immunoreactivity compared to WT mice (Fig. 2b). In addition, the glomeruli diameters were measured to quantify the OSN density as an indirect indicator of total OSNs numbers. The diameters in GluN3A KO mice were significantly lower than that in WT mice (Fig. 2c). Western blot analysis consistently showed lower expression of OMP protein in the olfactory bulb from GluN3A KO mice (Fig. 2d, e).

In the WT mouse, GluN3A immunoreactivity was detected in the olfactory epithelium (Fig. 3a). GluN3A expression mainly existed in the olfactory sensory neurons (OSNs), which are located in the olfactory epithelium in the nasal cavity. However, GluN3A KO mice exhibited scant GluN3A immunoreactivity. OMP immunoreactivity was also expressed on the membranes of the cilia (Fig. 3a). Consistent with the results from the olfactory bulb, GluN3A KO mice had fewer OSN cells and exhibited the lower expression of OMP immunoreactivity in the olfactory epithelium than that in WT mice (Fig. 3a). This was supported by results of cell counting of OSN neurons in the epithelium stained with Hoechst 33342 in KO mice (Fig. 3b). In addition, we also measured the glomeruli diameter (Fig. 2c). Both results demonstrated significantly lower expression of OMP as well as a lower number of OSN. Western blot analysis confirmed significantly lower levels of OMP in the olfactory epithelium compared to WT mice (Fig. 3c, d). These observations on the changes in the expression of OMP implied that deletion of GluN3A resulted in fewer numbers of mature OSNs and impaired olfactory signaling transduction.

c-Fos expression in the olfactory system of WT and GluN3A KO mice

Induction of immediate-early genes such as c-Fos has been used as a marker of neuronal responses to stress stimuli (Dragunow and Faull 1989; Hoffman et al. 1993). In the olfactory system, c-Fos expression in responding to odor stimuli has been used as an indicator of olfactory activity in the olfactory bulb and epithelium (Herdegen and Leah 1998; Norlin et al. 2005; Guthrie et al. 1993). As a step to delineate the functional role of GluN3A in olfaction, we analyzed c-Fos expression in response to a butyl alcohol olfactory stimulus. The olfactory bulb and epithelium in WT and GluN3A mice normally had little expression of c-Fos (Figs. 4a, 5a). After exposure to butyl alcohol, c-Fos expression increased in the olfactory bulb and epithelium of both WT and GluN3A KO mice. Similarly like previously reported, c-Fos upregulation in the olfactory epithelium was less evident than that occurred in olfactory bulb (Figs. 4a, 5a) (Norlin et al. 2005). Immunoreactivity of



c-Fos was detected mainly in MCL and GCL of the olfactory bulb and in scattered OSNs of the olfactory epithelium (Figs. 4a, b, 5a). Although the expression of c-Fos in GL was detectable, the expression patterns were similar between WT and GluN3A KO mice upon butyl alcohol exposure (data not shown). Importantly, GluN3A

KO mice showed lower c-Fos expression than WT mice in both olfactory bulb and epithelium after butyl alcohol exposure. In Western blotting assays, c-Fos protein expression was consistently lower in GluN3A KO mice compared with that in WT mice in both olfactory bulb and epithelium after butyl alcohol exposure (Figs. 4c, d, 5b, c).

Fig. 1 GluN3A expression patterns in the olfactory bulb of WT and GluN3A KO mice. Immunohistochemistry illustrated the localization of GluN3A expression at the cellular level in the olfactory bulb of adult WT mice. **a** Representative images of GluN3A immunoreactivity (green) in the olfactory bulb. The image on the left shows an olfactory bulb. The right images at high magnification show high levels of GluN3A immunoreactivity in the granular cell layer (GCL), mitral cell layer (MCL), and glomerular layer (GL) in the olfactory bulb. Blue color is Hoechst 33342 staining. Scale bars 100 μ m. **b** Representative image showed co-labeling of NeuN (red) and GluN3A (green) in the GCL and MCL regions of olfactory bulb from WT brain, suggesting GluN3A is expressed in neurons. Blue color is Hoechst 33342 staining. Scale bars 20 μ m. **c** The same immunohistochemical staining as in **a** performed in the GluN3A KO brain. In a striking difference from **a**, GluN3A immunoreactivity (green) was absent in different areas of the olfactory bulb. Blue color is Hoechst 33342 staining. The dotted line in the high magnification images of **a** and **c** were drawn along the edge of Hoechst 33342 staining to illustrate the boundaries between different regions. Scale bars 100 μ m. **d, e** Representative Western blot results of the expressions of several NMDAR subunits (**d**) and GluN3A expression in WT and GluN3A KO olfactory bulbs. **f–i** Quantified Western blot results of the expression of major NMDAR subunits in the olfactory bulb from WT and GluN3A KO mice. The expression levels of NMDAR subunit GluN1, GluN2B, and GluN3B were similar in WT and GluN3A KO mice, while GluN3A expression was barely detectable in KO mice. $n = 6$ per group

CaMKII and CREB expressions in olfactory bulb in WT and GluN3A KO mice

The Ca^{2+} - and calmodulin-dependent kinase II (CaMKII) is highly enriched at synapses and has been implicated in olfactory activities (Zou et al. 2002). For example, inhibiting CaMKII shows impaired odor perception (Leinders-Zufall et al. 1999). CaMKII can either stimulate or inhibit adenylyl cyclase in the olfactory system and regulate odor-stimulated cAMP induction (Wei et al. 1998; Zufall and Leinders-Zufall 2000). CaMKII inhibition leads to termination of olfactory signaling (Wei et al. 1998). In addition, cAMP response element-binding protein (CREB) can regulate the population of OSNs via the MAPK/CREB-dependent transcriptional pathway (Watt et al. 2004). CaMKII Immunoreactivity is observed in the EPL and GCL but minimal in the ONL and the GL (Neant-Fery et al. 2012). In Western blotting assays, the ratio of phosphorylated CaMKII/CaMKII protein expression was lower in GluN3A KO mice compared with WT mice (Fig. 6a–d). The expressions of CREB and phosphorylated CREB and the ratio of phosphorylated CREB/CREB were not significantly different between WT and GluN3A KO mice (Fig. 6a, e–g).

Impaired olfaction in GluN3A KO mice

We measured olfactory function using an established buried food-finding test (Yang and Crawley 2009). In this test,

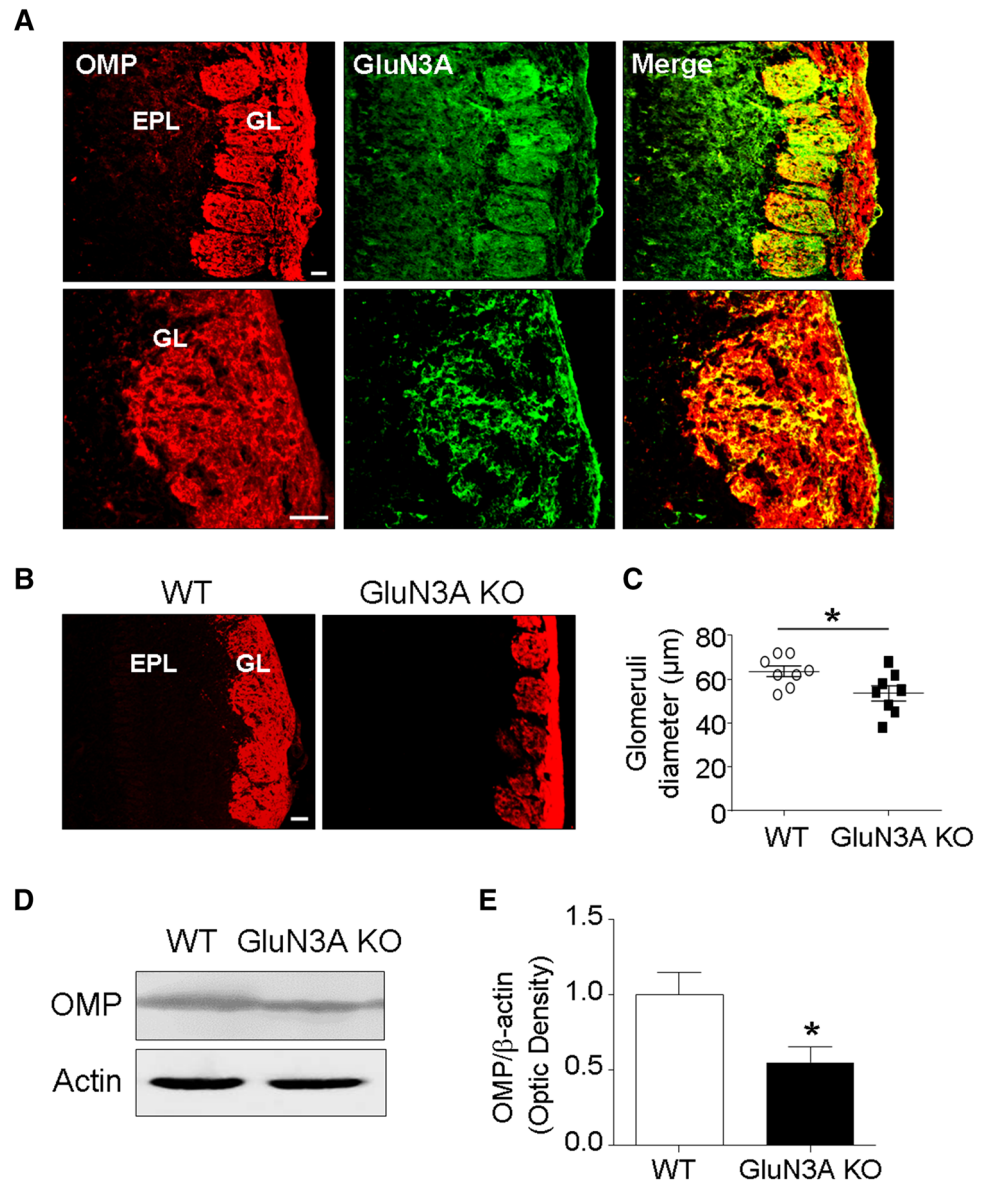
GluN3A KO mice took significantly longer distance to find buried food compared to WT mice (Fig. 7a). On the other hand, mice in both groups performed similarly in the visible food finding test (Fig. 7b). This result indicated that deleting GluN3A selectively affected olfactory but not visual function.

We previously reported that adult GluN3A KO mice walked slower than WT mice (Mohamad et al. 2013). This behavior may affect how fast the mice can reach to the buried food. In this investigation, we monitored the traveled distance and velocity using a Top Scan System during the buried food-finding test (Fig. 7c, d). During the test, GluN3A KO mice traveled longer distances and took longer time to find the buried food, but the average velocity within a 5 min period showed no significant difference between WT and KO groups (Fig. 7c, d). This measurement supported that although GluN3A KO mice might generally walk slower, this deficit was not strong enough to affect their walking behavior in searching for buried food in a nearby place.

The olfactory-specific function of odor discrimination was tested using olfactory habituation/dishabituation test (Fig. 8). In this test, presentation of a water-saturated cotton swab elicited an initial sniffing behavior but the response soon weakened in the subsequent second and third presentations of the water cotton (2 min intervals; habituation response). Following these water swab presentations, swabs saturated with chocolate extract (1:50 dilution) were presented and elicited significantly more sniffing responses than the water swab (dishabituation). The response decreased upon second and third presentations of the chocolate odor. The following presentations of three swabs saturated with imitation almond flavoring (1:200 dilution) elicited more sniffing that decreased again upon the second and third almond presentations. The habituation and dishabituation curves and the curve peaks showed sensory abilities to detect and discriminate between odors. Both WT and GluN3A KO mice decreased the number of sniffing similarly when they were exposed to second or third presentations of the same odor. However, GluN3A KO mice had lower sniffing time when different odors were presented (Fig. 8).

To test and confirm the olfactory deficits in GluN3A KO mice, we further examined the sniffing behavior in their natural environment using a home cage monitoring system (Fig. 7e). This video-based platform provides automated high-resolution behavior monitoring and analysis (Steele et al. 2007; Lee et al. 2014). It was clear that GluN3A mice showed low bouts of sniffing compared with WT mice during the surveillance of 24 h. There was no difference in bouts of chewing behavior between the two groups (Fig. 7f).

Fig. 2 GluN3A and OMP expression patterns in the olfactory bulbs of WT and GluN3A KO mice. The expression of GluN3A and olfactory marker protein (OMP) in the olfactory bulb was measured using Immunohistochemical and Western blot analyses. **a** In the GL of olfactory bulb in WT mice, GluN3A immunoreactivity (green) was colocalized with OMP expression (red). Scale bars 20 μm . **b** The brain section of olfactory bulb from WT and GluN3A KO mice of immunostaining using antibody against OMP (red). The OMP immunoreactivity was relatively higher in the GL, presumable in OSNs of the olfactory bulb. GluN3A KO mice exhibited lower expression of OMP immunoreactivity than WT mice. Scale bars 20 μm . **c** Significantly smaller glomeruli diameter was observed in GluN3A KO mice compare to WT mice. * $P < 0.05$ compared with WT; $n = 8$ per group. **d** and **e** Western blotting confirmed that the OMP expression was significantly attenuated in the olfactory bulb of GluN3A KO compared with that in WT mice. * $P < 0.05$ compared with WT; $n = 6$ per group



Discussion

Although the NMDA receptor subunit GluN3A or NR3A was discovered more than 10 years ago, its functional role has not been well understood. Due to its developmental changes from high expression at the neonatal stage to a relatively lower level in adult age (Wong et al. 2002), the significance of GluN3A expression in the adult brain has been largely ignored and mostly unknown. The present investigation reveals an important role of GluN3A in olfactory function in adult mice. We provide novel evidence that deletion of GluN3A results in down-regulation of the key olfactory marker OMP associated with mature OSNs in the olfactory bulb and olfactory epithelium. The up-regulation of the immediate-early gene *c-Fos* in response to butyl alcohol stimuli was attenuated in

GluN3A KO mice. In the absence of GluN3A, animals had difficulties in locating buried food while their vision function was normal. Consistently, odor distinguishable abilities of GluN3A KO mice were lower comparing to WT mice. These findings suggest that GluN3A expressed in the olfactory system plays a significant role in regulating odor detection and discrimination abilities in adult mice.

It is well known that GluN3A expression reaches to its peak level during the early postnatal days and its level subsides into adulthood. Nevertheless, our investigations demonstrate that this developmental change does not mean GluN3A in the adult brain can be less important (Mohamad et al. 2013; Lee et al. 2015). We recently reported that adult GluN3A KO mice showed enhanced recognition and spatial learning and memory functions. Hippocampal slices from juvenile and adult GluN3A KO mice exhibited

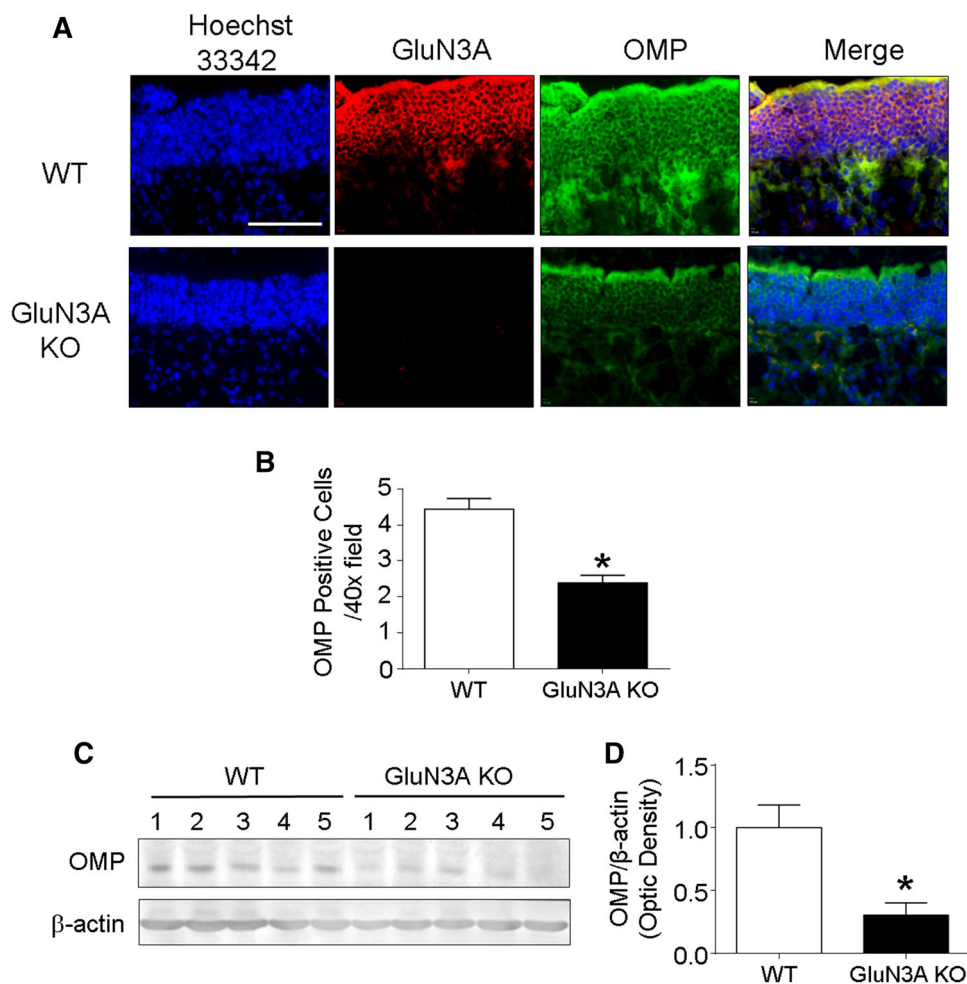


Fig. 3 GluN3A and OMP expression patterns in the olfactory epithelium from WT and GluN3A KO mice. Immunohistochemical and Western blot analyses revealed the expression of GluN3A and olfactory marker protein (OMP) in the olfactory epithelium. **a** GluN3A and OMP expressions were examined in the olfactory epithelium using immunohistochemical staining. GluN3A immunoreactivity (*red*) was mainly detected in the olfactory sensory neurons in WT mice, which was confirmed by the expression pattern of OMP (*green*). Hoechst 33342 staining (*blue*) shows the olfactory epithelium

cells. Both GluN3A and OMP immunoreactivities were greatly diminished in the GluN3A KO mice. *Scale bars* 100 μ m. **b** Quantified data from the immunostaining data in **a**; in the olfactory epithelium, the number of OMP-positive cells in WT mice was significantly higher than that in GluN3A KO mice. **c** and **d** Western blot analysis revealed the different expression levels of OMP in the olfactory epithelium. GluN3A KO mice had significantly low expression level of OMP compared with WT mice. * $P < 0.05$ compared with WT, $n = 5$ per group

greater LTP compared with WT slices (Mohamad et al. 2013). An elevated level of CaMKII and the increased phosphorylated CaMKII level upon LTP induction were identified as a molecular mechanism underlying the enhanced LTP and cognitive function. Unlike the previous observation in the hippocampus, we now detected reduced expression of CaMKII in the olfactory bulb and diminished olfactory activity. CaMKII is expressed in the GABAergic granule cells in the olfactory bulb and involved in regulating odor adaptation in olfaction via OSNs (Wei et al. 1998; Leinders-Zufall et al. 1999; Zou et al. 2002). Lower CaMKII expression in the olfactory bulb is consistent with impaired olfactory function in GluN3A KO mice. Considering previous and current investigations, it is suggested

that deleting GluN3A may cause hyper- or hypo-activity in the adult brain, depending on the relative basal level of the subunit and on the NMDAR-associated regulatory pathways.

An important finding of this study is that GluN3A KO mice have low levels of OMP expression in both the olfactory bulb and olfactory epithelium compared to WT mice. OMP is a 19-kDa phylogenetically conserved cytoplasmic protein that is expressed exclusively by mature OSNs in vertebrate species (Buiakova et al. 1996; Lee et al. 2011). Previous animal studies have indicated that OMP expression in the olfactory system modulates odor detection and the signal transduction cascade in OSNs (Buiakova et al. 1996). Previous studies using OMP-deficient

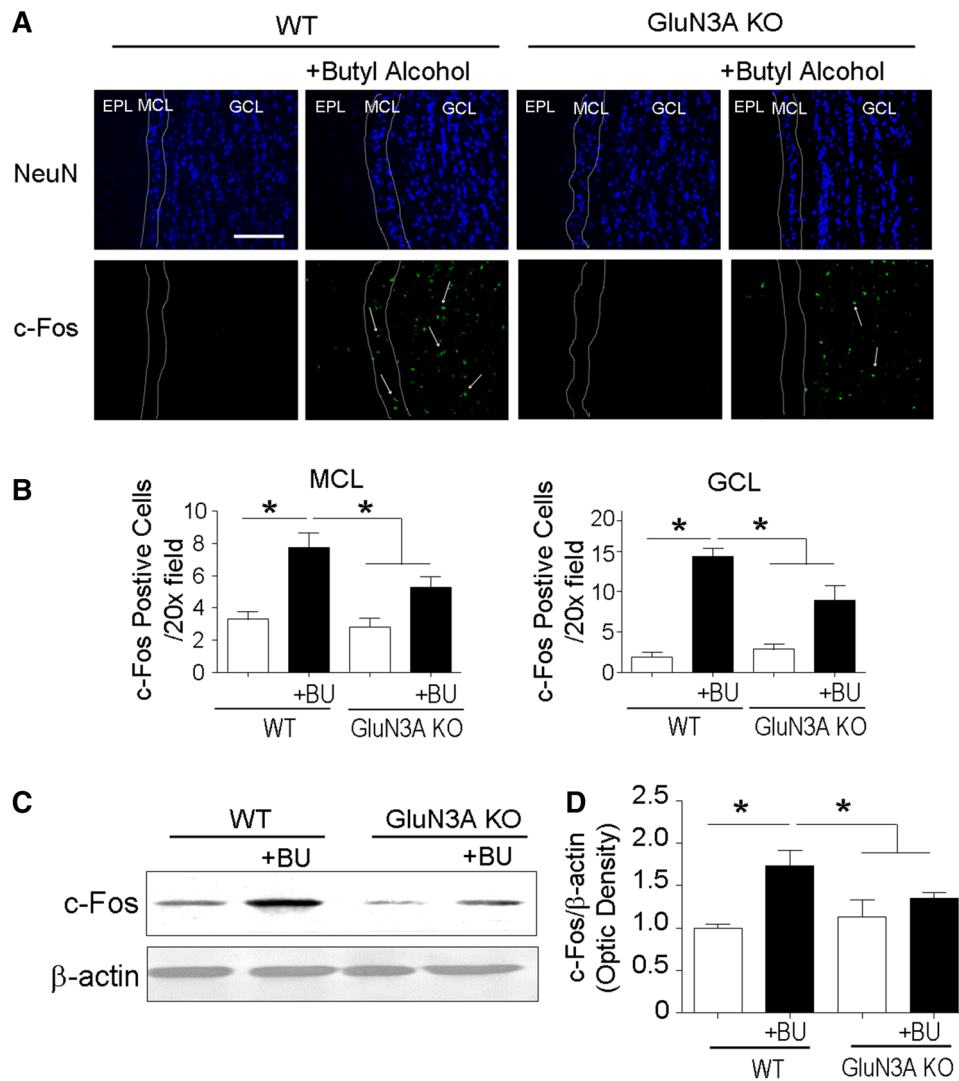


Fig. 4 c-Fos expression in the olfactory bulb of WT and GluN3A KO mice. c-Fos expression in the olfactory bulb after exposure to butyl alcohol was analyzed to investigate the effect of GluN3A expression on early olfactory response. **a** Immunohistochemical staining of the olfactory bulb from WT and GluN3A KO mice. NeuN staining revealed the cell distributions and cellular layers. The dotted lines in images were drawn along the edges of NeuN staining to illustrate the boundaries between different regions marked in the images. Little expression of c-Fos was detected without olfactory stimulation in either WT or KO mice. After exposure to butyl alcohol (BU),

increased c-Fos expression was observed in the olfactory bulbs of WT, but much lower c-Fos response was seen in GluN3A KO mice. *Arrow* indicates examples of c-Fos-positive cells. *Scale bars* 100 μ m. $*P < 0.05$; $n = 6$ per group. **b** Quantified data from the immunostaining data in **a**; in the MCL and GCL regions, the number of c-Fos-positive cells in WT mice was significantly higher than that in GluN3A KO mice. **c**, **d** Western blot analysis confirmed that the increase in c-Fos expression in responding to butyl alcohol stimulus was basically absent in GluN3A KO mice. $*P < 0.05$ compared to WT, $n = 6$ per group

mice (OMP KO) showed low electroolfactogram (EOG) response of olfactory epithelium after exposure to several odorants, altered kinetics of response generation and recovery, and a reduced ability to respond to the second odor stimulation (Youngentob et al. 2003). These results imply that, in OMP-deficient mice, there is an overall reduction of neuronal activity in the olfactory projection to the olfactory bulb. In addition, reducing OMP expression by toxins such as 3-methylindole can lead to olfactory impairments (Kim et al. 2010). These results strongly

support the idea that olfactory activity is correlated with the relative density of OMP expression in the olfactory bulb and olfactory epithelium. Furthermore, the OMP expression level appears to correlate with the neuronal population because all mature OSNs express OMP (Danciger et al. 1989). It is possible that deletion or deficiency of GluN3A may cause deficits in the production of mature OSNs and abnormal olfactory activity.

OSNs can bind to a variety of odor molecules in the olfactory epithelium of the nasal cavity, leading to the

Fig. 5 c-Fos expression in olfactory epithelium in WT and GluN3A KO mice. c-Fos expression in the olfactory epithelium in responding to butyl alcohol was examined in WT and GluN3A KO mice. **a** Hoechst 33342 staining (blue) shows the olfactory epithelium cells. Immunoreactivity of c-Fos (green) was detected in the olfactory epithelium. Following butyl alcohol exposure, c-Fos expression was increased in WT mice but much less obvious in GluN3A KO mice. Scale bars 50 μ m. **b, c** Western blot analysis revealed that c-Fos expression was significantly lower in GluN3A KO mice compared with WT mice and the response to butyl alcohol (BU) was diminished in these animals. * $P < 0.05$, $n = 6$ per group

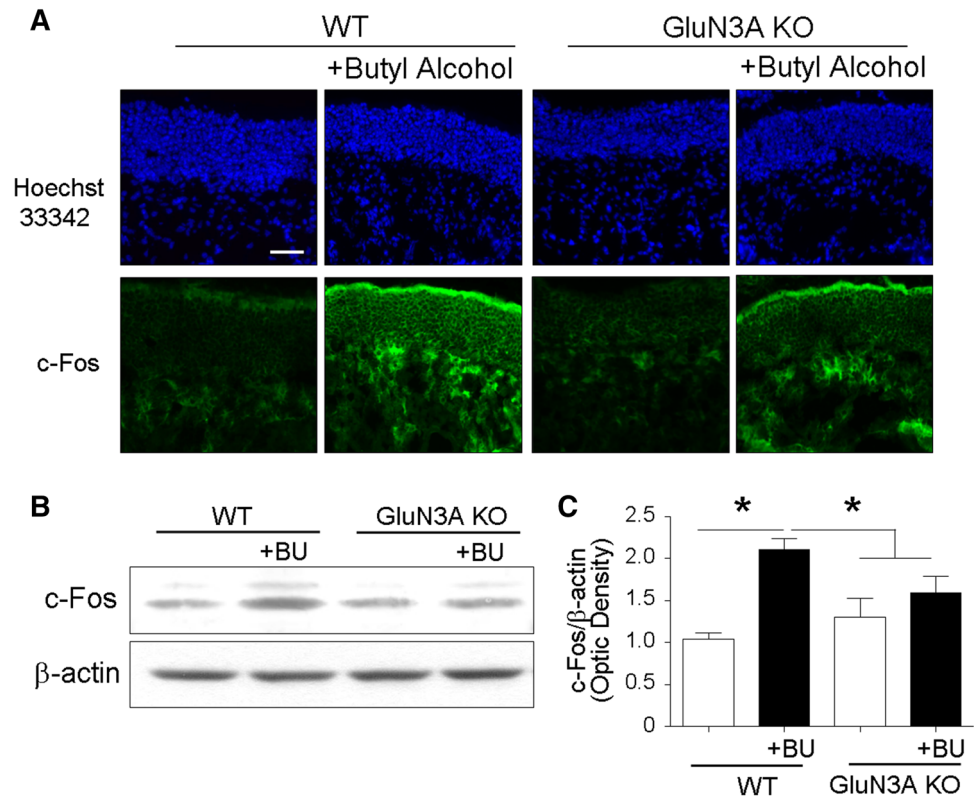
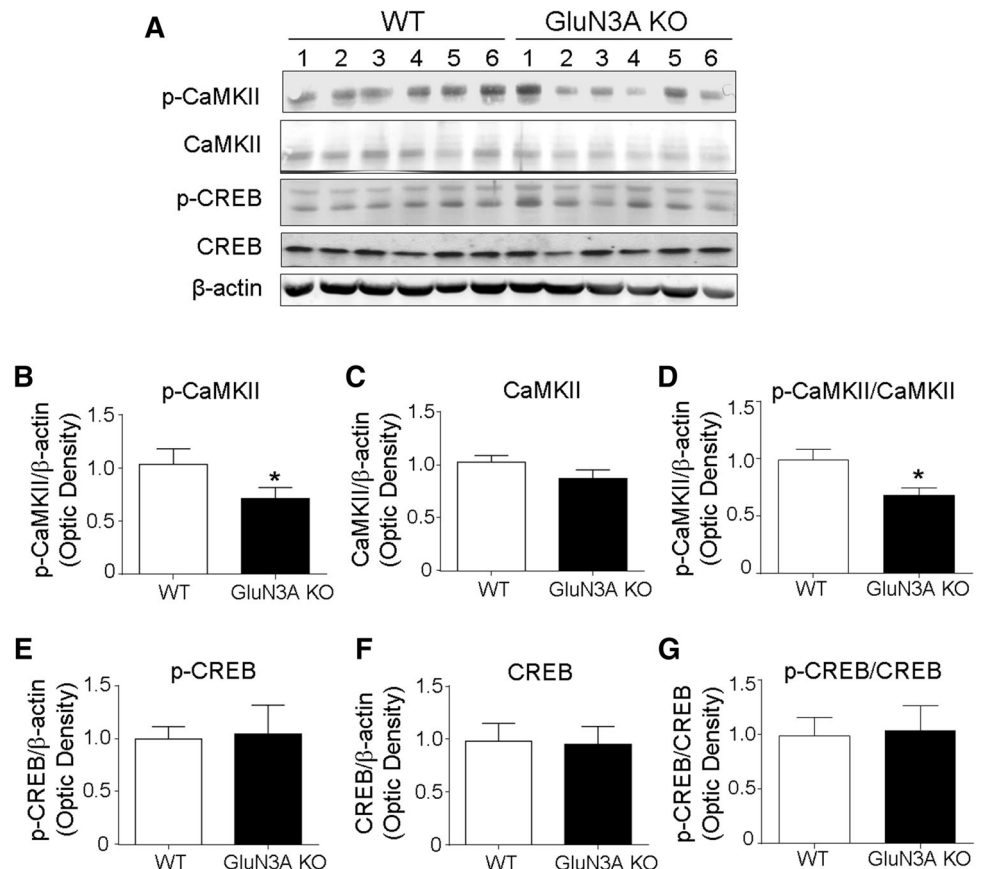


Fig. 6 CaMKII and CREB expressions in the olfactory bulb of WT and GluN3A KO mice. CaMKII and CREB, which are highly enriched in olfactory bulb, regulate the odor-stimulated cAMP induction and the population of OSNs, implicating the odor perception of the olfactory system. The expressions of CaMKII and CREB were examined using Western blotting in the olfactory bulb. **a–g** Expression levels of CaMKII and CREB were measured using Western blot analysis in the olfactory bulb from WT and GluN3A KO mice. Phosphorylated CaMKII (p-CaMKII) was significantly reduced in GluN3A KO mice, while CaMKII, p-CREB, CREB, and p-CREB/CREB were similarly expressed in the olfactory bulb of WT and GluN3A KO mice. In addition, the ratio of p-CaMKII/CaMKII was significantly lower in GluN3A KO mice. * $P < 0.05$, $n = 6$ per group



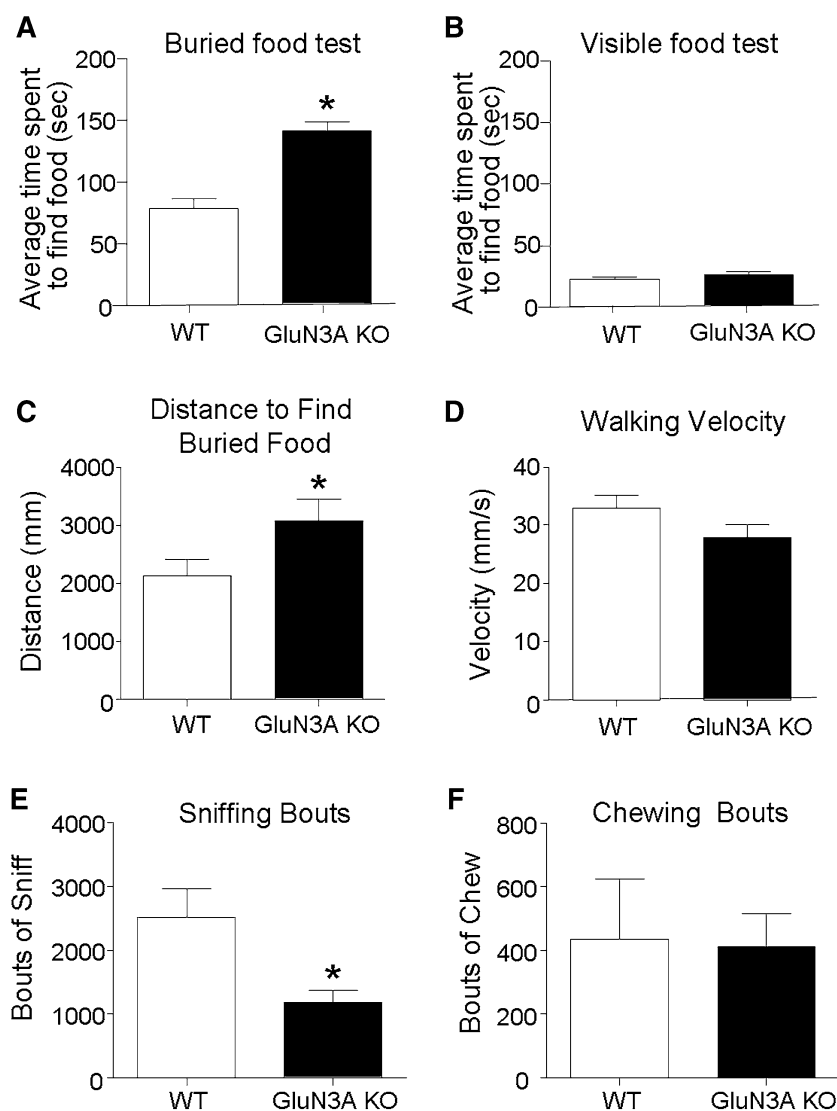


Fig. 7 Impaired olfaction of GluN3A KO mice. Olfactory behaviors were compared between adult WT and GluN3A KO mice. **a** In the buried food finding test, the latency to find a buried food was measured. GluN3A KO mice spent significantly longer time to locate buried food than WT mice. $*P < 0.05$ versus WT mice; $n = 28$ and 31 in WT and GluN3A KO groups. **b** As a control, the visible food-finding test showed that WT and GluN3A KO mice spent similar time finding visible food. $n = 16$ and 17 in WT and GluN3A KO groups. **c** In the buried food-finding test, GluN3A KO mice traveled significantly more distance before locating the food compared to WT mice. $*P < 0.05$ versus WT mice; $n = 16$ and 17 in WT and

GluN3A KO groups. **d** The walking velocity of animals during the food finding tests, measured using a top scan camera. GluN3A KO showed a trend of reduced walking speed although the difference was not statistically significant in these experiments. $n = 16$ and 17 in WT and GluN3A KO groups. **e** Home Cage monitoring systems were used to monitor and analyze behavioral patterns of WT and GluN3A KO mice. During the 24-h surveillance in the home cages environment, significantly low bouts of sniffing were observed in GluN3A KO mice compared with WT mice. $*P < 0.05$ versus WT mice; $n = 12$ per group. **f** The bouts of chewing activity were not different between the two groups. $n = 12$ per group

intracellular G-protein, production of cyclic AMP (cAMP) and activation of ion channels in the cell membrane, resulting in regulating the odor perception via generation of action potentials (Fan and Ngai 2001; Bieri et al. 2004). In this current study, we observed that GluN3A expression mainly existed in the OSNs in the olfactory epithelium. Therefore, these findings suggest that the expression of GluN3A in the olfactory structure can be an important

regulator mediating odor perception in the olfactory system.

To determine whether GluN3A expression can affect olfaction, we measured the expression of c-Fos, an immediate-early gene, in the olfactory bulb and olfactory epithelium. c-Fos expression has been used to evaluate the coordination of OSNs by exposure to odors in rodents (Guthrie et al. 1993; Norlin et al. 2005). Expression of

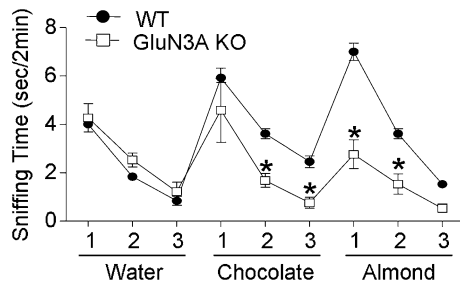


Fig. 8 Olfactory habituation/dishabituation test. The olfactory habituation/dishabituation test was performed to test whether the animal's function of detecting and differentiating different odors. We presented 3 odors (water, chocolate, and almond) to WT and GluN3A KO mice 3 times each, and the bouts of sniffing were counted. Although WT and GluN3A KO mice showed similar decreases in sniffing activities after repeated water presentations, the bouts of sniffing after the odorant exposures to chocolate and almond were significantly reduced in GluN3A KO mice compared to that of WT mice. The initial response to the first presentation of almond was also greatly reduced in GluN3A KO mice. * $P < 0.05$ versus WT mice; $n = 13$ –14 per group

c-Fos can be rapidly induced by extracellular stimulation such as Ca^{2+} -mediated depolarization after exposure to odors (Guthrie et al. 1993). Also, changing levels of c-Fos expression have been shown to regulate NMDA-mediated synaptic plasticity (Lethbridge et al. 2012). GluN3A assembles with other NMDAR subunits to form functional receptors (Dingledine et al. 1999; Al-Hallaq et al. 2002). In the current study, both WT and GluN3A KO mice had little constitutive expression of c-Fos in the olfactory bulb. However, WT mice responded to butyl alcohol stimuli with increased expressions of c-Fos in GL, MCL, and GCL regions of the olfactory system, indicating that direct and indirect stimulation could be activated after exposure to butyl alcohol. Although the expression of c-Fos showed similar patterns between WT and GluN3A KO mice upon butyl alcohol exposure in GL, the activation of its expression in MCL and GCL was much weaker in GluN3A KO mice. The role of immediate-early genes and possible involvement of Ca^{2+} homeostasis in the regulation of olfactory function remains to be elucidated.

Odor is detected and discriminated through brief bouts of sniffing and involves odor information processing in the olfactory bulb (Youngentob et al. 1987; Wesson et al. 2008). The bouts of sniffing have been used as a reliable indicator of olfaction (Chaudhury et al. 2010; Witt et al. 2009). In the current study, GluN3A KO mice showed low bouts of sniffing in olfactory habituation/dishabituation tests. In addition, the home cage behavioral analysis of sniffing activity under natural environment further verified the finding that GluN3A KO mice show deficient olfactory activity. On the other hand, the bouts of chewing activity and visible food finding test detected no difference between

groups, suggesting the specificity of GluN3A expression in regulating olfactory functions.

In the present investigation, GluN3A conventional KO mice were tested. It was possible that the observed functional deficits due to the absence of this subunit in other brain regions might also contribute to the observed dysfunction. Moreover, the timing of eliminating GluN3A may be another factor for the changes in the adult brain. In other words, the observation in the adults KO mice could be due to abnormal brain development during early stages. For example, deletion of GluN3A increased dendritic spine densities in the early postnatal cerebrocortical neurons (Das et al. 1998). During brain development, the elimination of GluN3A results in a mature synaptic organization characterized by more synapses and larger postsynaptic densities (Henson et al. 2012; Roberts et al. 2009). Recent evidence suggests that the GluN3A subunit enables presynaptic NMDARs to regulate spontaneous and evoked glutamate release (Larsen et al. 2011). As in the current investigation, conventional GluN3A KO mice were used in that report and the effect was observed at juvenile age. In future investigations, conditional/inducible knockout and/or knockdown of this NMDAR subunit may be needed to clarify the timing issue for the changes in adult and juvenile brains.

In conclusion, the present investigation on adult GluN3A KO mice provides new insights into a previously unknown role of this subunit in olfactory function. GluN3A KO mice exhibited impaired olfactory activity characterized by longer time needed for finding buried food, associated with a reduced ability to respond to an odor stimulus, and deficient olfactory-related behaviors. Low OMP expression was detected in the olfactory system of GluN3A KO mice, suggesting a deficit in the mature OSN population. The specialized spatial expressions of c-Fos following exposure to odor indicated that GluN3A expression was involved in not only odor detection, but also odor information transferring of the olfactory bulb. Although further study is needed to better understand the role of GluN3A in olfaction, these initial observations are consistent with the conclusion that GluN3A in the adult brain can be a novel modulator of NMDAR-mediated odor detection and the transduction of odor information.

Acknowledgments This work was supported by the NIH grants NS0458710 (SPY), NS075338 (LW), NS062097 (LW), NS073378 (TAD and SPY), and the American Heart Association grant AHA 12GRNT12060222 (SPY) and the AHA Established Investigator Award (LW).

Compliance with ethical standards

Conflict of interest None.

Research involving Human Participants and/or Animals No human participants involved. All animal experiments and experimental protocols were approved by the Emory University Institutional Animal Care and Use Committee (IACUC) and were in compliance with National Institutes of Health (NIH) guidelines.

References

- Al-Hallaq RA, Jarabek BR, Fu Z, Vicini S, Wolfe BB, Yasuda RP (2002) Association of NR3A with the *N*-methyl-D-aspartate receptor NR1 and NR2 subunits. *Mol Pharmacol* 62(5):1119–1127
- Baldisseri DM, Margolis JW, Weber DJ, Koo JH, Margolis FL (2002) Olfactory marker protein (OMP) exhibits a beta-clam fold in solution: implications for target peptide interaction and olfactory signal transduction. *J Mol Biol* 319(3):823–837. doi:10.1016/S0022-2836(02)00282-6
- Bieri S, Monastyrskaia K, Schilling B (2004) Olfactory receptor neuron profiling using sandalwood odorants. *Chem Senses* 29(6):483–487. doi:10.1093/chemse/bjh050
- Bliss TV, Collingridge GL (1993) A synaptic model of memory: long-term potentiation in the hippocampus. *Nature* 361(6407):31–39. doi:10.1038/361031a0
- Buiakova OI, Baker H, Scott JW, Farbman A, Kream R, Grillo M, Franzen L, Richman M, Davis LM, Abbondanzo S, Stewart CL, Margolis FL (1996) Olfactory marker protein (OMP) gene deletion causes altered physiological activity of olfactory sensory neurons. *Proc Natl Acad Sci USA* 93(18):9858–9863
- Chaudhury D, Manella L, Arellanos A, Escanilla O, Cleland TA, Linster C (2010) Olfactory bulb habituation to odor stimuli. *Behav Neurosci* 124(4):490–499. doi:10.1037/a0020293
- Chen WR, Xiong W, Shepherd GM (2000) Analysis of relations between NMDA receptors and GABA release at olfactory bulb reciprocal synapses. *Neuron* 25(3):625–633. pii S0896-6273(00)81065-X
- Choi DW (1992) Excitotoxic cell death. *J Neurobiol* 23(9):1261–1276. doi:10.1002/neu.480230915
- Ciabarra AM, Sullivan JM, Gahn LG, Pecht G, Heinemann S, Sevarino KA (1995) Cloning and characterization of chi-1: a developmentally regulated member of a novel class of the ionotropic glutamate receptor family. *J Neurosci* 15(10):6498–6508
- Cull-Candy S, Brickley S, Farrant M (2001) NMDA receptor subunits: diversity, development and disease. *Curr Opin Neurobiol* 11(3):327–335
- Danciger E, Mettling C, Vidal M, Morris R, Margolis F (1989) Olfactory marker protein gene: its structure and olfactory neuron-specific expression in transgenic mice. *Proc Natl Acad Sci USA* 86(21):8565–8569
- Das S, Sasaki YF, Rothe T, Premkumar LS, Takasu M, Crandall JE, Dikkes P, Conner DA, Rayudu PV, Cheung W, Chen HS, Lipton SA, Nakanishi N (1998) Increased NMDA current and spine density in mice lacking the NMDA receptor subunit NR3A. *Nature* 393(6683):377–381. doi:10.1038/30748
- Dingledine R, Borges K, Bowie D, Traynelis SF (1999) The glutamate receptor ion channels. *Pharmacol Rev* 51(1):7–61
- Dragunow M, Faull R (1989) The use of c-fos as a metabolic marker in neuronal pathway tracing. *J Neurosci Met* 29(3):261–265
- Fan J, Ngai J (2001) Onset of odorant receptor gene expression during olfactory sensory neuron regeneration. *Dev Biol* 229(1):119–127. doi:10.1006/dbio.2000.9972
- Firestein S (2001) How the olfactory system makes sense of scents. *Nature* 413(6852):211–218. doi:10.1038/35093026
- Guthrie KM, Anderson AJ, Leon M, Gall C (1993) Odor-induced increases in c-fos mRNA expression reveal an anatomical “unit” for odor processing in olfactory bulb. *Proc Natl Acad Sci USA* 90(8):3329–3333
- Halabisky B, Friedman D, Radojicic M, Strowbridge BW (2000) Calcium influx through NMDA receptors directly evokes GABA release in olfactory bulb granule cells. *J Neurosci* 20(13):5124–5134. pii 20/13/5124
- Henson MA, Larsen RS, Lawson SN, Perez-Otano I, Nakanishi N, Lipton SA, Philpot BD (2012) Genetic deletion of NR3A accelerates glutamatergic synapse maturation. *PLoS One* 7(8):e42327. doi:10.1371/journal.pone.0042327
- Herdegen T, Leah JD (1998) Inducible and constitutive transcription factors in the mammalian nervous system: control of gene expression by Jun, Fos and Krox, and CREB/ATF proteins. *Brain Res Brain Res Rev* 28(3):370–490
- Hoffman GE, Smith MS, Verbalis JG (1993) c-Fos and related immediate early gene products as markers of activity in neuroendocrine systems. *Front Neuroendocrinol* 14(3):173–213. doi:10.1006/frne.1993.1006
- Hollmann M, Heinemann S (1994) Cloned glutamate receptors. *Annu Rev Neurosci* 17:31–108. doi:10.1146/annurev.ne.17.030194.000335
- Isaacson JS (2001) Mechanisms governing dendritic gamma-aminobutyric acid (GABA) release in the rat olfactory bulb. *Proc Natl Acad Sci USA* 98(1):337–342. doi:10.1073/pnas.021445798
- Isaacson JS, Strowbridge BW (1998) Olfactory reciprocal synapses: dendritic signaling in the CNS. *Neuron* 20(4):749–761. pii S0896-6273(00)81013-2
- Jamain S, Radyushkin K, Hammerschmidt K, Granon S, Boretius S, Varoqueaux F, Ramanantsoa N, Gallego J, Ronnenberg A, Winter D, Frahm J, Fischer J, Bourgeron T, Ehrenreich H, Brose N (2008) Reduced social interaction and ultrasonic communication in a mouse model of monogenic heritable autism. *Proc Natl Acad Sci USA* 105(5):1710–1715. doi:10.1073/pnas.0711555105
- Kim JW, Hong SL, Lee CH, Jeon EH, Choi AR (2010) Relationship between olfactory function and olfactory neuronal population in C57BL/6 mice injected intraperitoneally with 3-methylindole. *Otolaryngol Head Neck Surg* 143(6):837–842. doi:10.1016/j.otohns.2010.08.016
- Larsen RS, Corlew RJ, Henson MA, Roberts AC, Mishina M, Watanabe M, Lipton SA, Nakanishi N, Perez-Otano I, Weinberg RJ, Philpot BD (2011) NR3A-containing NMDARs promote neurotransmitter release and spike timing-dependent plasticity. *Nat Neurosci* 14(3):338–344. doi:10.1038/nn.2750
- Laurie DJ, Seeburg PH (1994) Regional and developmental heterogeneity in splicing of the rat brain NMDAR1 mRNA. *J Neurosci* 14(5 Pt 2):3180–3194
- Lee AC, He J, Ma M (2011) Olfactory marker protein is critical for functional maturation of olfactory sensory neurons and development of mother preference. *J Neurosci* 31(8):2974–2982. doi:10.1523/JNEUROSCI.5067-10.2011
- Lee J, Gu X, Wei L, Wei Z, Dix TA, Yu SP (2014) Therapeutic effects of pharmacologically induced hypothermia against traumatic brain injury in mice. *J Neurotrauma*. doi:10.1089/neu.2013.3251
- Lee JH, Wei ZZ, Chen D, Gu X, Wei L, Yu SP (2015) A neuroprotective role of the NMDA receptor subunit GluN3A (NR3A) in ischemic stroke of the adult mouse. *Am J Physiol Cell Physiol* 308(7):C570–C577. doi:10.1152/ajpcell.00353.2014
- Leinders-Zufall T, Ma M, Zufall F (1999) Impaired odor adaptation in olfactory receptor neurons after inhibition of Ca²⁺/calmodulin kinase II. *J Neurosci* 19(14):RC19

- Lethbridge R, Hou Q, Harley CW, Yuan Q (2012) Olfactory bulb glomerular NMDA receptors mediate olfactory nerve potentiation and odor preference learning in the neonate rat. *PLoS One* 7(4):e35024. doi:[10.1371/journal.pone.0035024](https://doi.org/10.1371/journal.pone.0035024)
- Margot C (2009) A noseful of objects. *Nat Neurosci* 12(7):813–814. doi:[10.1038/nn0709-813](https://doi.org/10.1038/nn0709-813)
- McBain CJ, Mayer ML (1994) *N*-methyl-D-aspartic acid receptor structure and function. *Physiol Rev* 74(3):723–760
- Meldrum BS (2000) Glutamate as a neurotransmitter in the brain: review of physiology and pathology. *J Nutr* 130(4S Suppl):1007S–1015S
- Mohamad O, Song M, Wei L, Yu SP (2013) Regulatory roles of the NMDA receptor GluN3A subunit in locomotion, pain perception and cognitive functions in adult mice. *J Physiol* 591(Pt 1):149–168. doi:[10.1113/jphysiol.2012.239251](https://doi.org/10.1113/jphysiol.2012.239251)
- Monyer H, Sprengel R, Schoepfer R, Herb A, Higuchi M, Lomeli H, Burnashev N, Sakmann B, Seeburg PH (1992) Heteromeric NMDA receptors: molecular and functional distinction of subtypes. *Science* 256(5060):1217–1221
- Neant-Fery M, Peres E, Nasrallah C, Kessner M, Gribaudo S, Greer C, Didier A, Trembleau A, Caille I (2012) A role for dendritic translation of CaMKIIalpha mRNA in olfactory plasticity. *PLoS One* 7(6):e40133. doi:[10.1371/journal.pone.0040133](https://doi.org/10.1371/journal.pone.0040133)
- Norlin EM, Vedin V, Bohm S, Berghard A (2005) Odorant-dependent, spatially restricted induction of c-fos in the olfactory epithelium of the mouse. *J Neurochem* 93(6):1594–1602. doi:[10.1111/j.1471-4159.2005.03159.x](https://doi.org/10.1111/j.1471-4159.2005.03159.x)
- Pabba M, Hristova E, Biscaro D (2012) The elusive roles of NMDA receptor amino-terminal domains. *J Physiol* 590(Pt 22):5561–5562. doi:[10.1113/jphysiol.2012.243311](https://doi.org/10.1113/jphysiol.2012.243311)
- Perez-Otano I, Schulteis CT, Contractor A, Lipton SA, Trimmer JS, Sucher NJ, Heinemann SF (2001) Assembly with the NR1 subunit is required for surface expression of NR3A-containing NMDA receptors. *J Neurosci* 21(4):1228–1237
- Roberts AC, Diez-Garcia J, Rodriguiz RM, Lopez IP, Lujan R, Martinez-Turrillas R, Pico E, Henson MA, Bernardo DR, Jarrett TM, Clendeninn DJ, Lopez-Mascaraque L, Feng G, Lo DC, Wesseling JF, Wetsel WC, Philpot BD, Perez-Otano I (2009) Downregulation of NR3A-containing NMDARs is required for synapse maturation and memory consolidation. *Neuron* 63(3):342–356. doi:[10.1016/j.neuron.2009.06.016](https://doi.org/10.1016/j.neuron.2009.06.016)
- Schoppa NE, Kinzie JM, Sahara Y, Segerson TP, Westbrook GL (1998) Dendrodendritic inhibition in the olfactory bulb is driven by NMDA receptors. *J Neurosci* 18(17):6790–6802
- Shepherd GM (2004) *The synaptic organization of the brain*, 5th edn. Oxford University Press, Oxford, New York
- Smith PC, Firestein S, Hunt JF (2002) The crystal structure of the olfactory marker protein at 2.3 Å resolution. *J Mol Biol* 319(3):807–821. doi:[10.1016/S0022-2836\(02\)00242-5](https://doi.org/10.1016/S0022-2836(02)00242-5)
- Steele AD, Jackson WS, King OD, Lindquist S (2007) The power of automated high-resolution behavior analysis revealed by its application to mouse models of Huntington's and prion diseases. *Proc Natl Acad Sci USA* 104(6):1983–1988. doi:[10.1073/pnas.0610779104](https://doi.org/10.1073/pnas.0610779104)
- Sucher NJ, Akbarian S, Chi CL, Leclerc CL, Awobuluyi M, Deitcher DL, Wu MK, Yuan JP, Jones EG, Lipton SA (1995) Developmental and regional expression pattern of a novel NMDA receptor-like subunit (NMDAR-L) in the rodent brain. *J Neurosci* 15(10):6509–6520
- Watt WC, Sakano H, Lee ZY, Reusch JE, Trinh K, Storm DR (2004) Odorant stimulation enhances survival of olfactory sensory neurons via MAPK and CREB. *Neuron* 41(6):955–967
- Wei J, Zhao AZ, Chan GC, Baker LP, Impey S, Beavo JA, Storm DR (1998) Phosphorylation and inhibition of olfactory adenylyl cyclase by CaM kinase II in Neurons: a mechanism for attenuation of olfactory signals. *Neuron* 21(3):495–504
- Wesson DW, Donahou TN, Johnson MO, Wachowiak M (2008) Sniffing behavior of mice during performance in odor-guided tasks. *Chem Senses* 33(7):581–596. doi:[10.1093/chemse/bjn029](https://doi.org/10.1093/chemse/bjn029)
- Witt RM, Galligan MM, Despinoy JR, Segal R (2009) Olfactory behavioral testing in the adult mouse. *J Vis Exp* 23:e949. doi:[10.3791/949](https://doi.org/10.3791/949)
- Wong HK, Liu XB, Matos MF, Chan SF, Perez-Otano I, Boyesen M, Cui J, Nakanishi N, Trimmer JS, Jones EG, Lipton SA, Sucher NJ (2002) Temporal and regional expression of NMDA receptor subunit NR3A in the mammalian brain. *J Comp Neurol* 450(4):303–317. doi:[10.1002/cne.10314](https://doi.org/10.1002/cne.10314)
- Yang M, Crawley JN (2009) Simple behavioral assessment of mouse olfaction. *Curr Protoc Neurosci* Chapter 8:Unit 8 24. doi:[10.1002/0471142301.ns0824s48](https://doi.org/10.1002/0471142301.ns0824s48)
- Youngentob SL, Mozell MM, Sheeha PR, Hornung DE (1987) A quantitative analysis of sniffing strategies in rats performing odor detection tasks. *Physiol Behav* 41(1):59–69
- Youngentob SL, Kent PF, Margolis FL (2003) OMP gene deletion results in an alteration in odorant-induced mucosal activity patterns. *J Neurophysiol* 90(6):3864–3873. doi:[10.1152/jn.00806.2002](https://doi.org/10.1152/jn.00806.2002)
- Zou DJ, Greer CA, Firestein S (2002) Expression pattern of alpha CaMKII in the mouse main olfactory bulb. *J Comp Neurol* 443(3):226–236
- Zufall F, Leinders-Zufall T (2000) The cellular and molecular basis of odor adaptation. *Chem Senses* 25(4):473–481